

Proceeding Paper

In Silico Evaluation of New Fluoroquinolones as Possible Inhibitors of Bacterial Gyrases in Resistant Gram-Negative Pathogens [†]

Manuel Alejandro Coba-Males ^{1,*}, Javier Santamaría-Aguirre ^{2,*} and Christian D. Alcívar-León ¹

¹ Facultad de Ciencias Químicas, Universidad Central del Ecuador, Quito 170521, Ecuador; cdalcivar@uce.edu.ec

² DNA Replication and Genome Instability Unit, Grupo de Investigación en Biodiversidad, Zoonosis y Salud Pública (GIBCIZ), Instituto de Investigación en Zoonosis-CIZ, Facultad de Ciencias Químicas, Universidad Central del Ecuador, Quito 170521, Ecuador

* Correspondence: macoba@uce.edu.ec (M.A.C.-M.); jrsantamaria@uce.edu.ec (J.S.-A.)

[†] Presented at the 25th International Electronic Conference on Synthetic Organic Chemistry, 15–30 November 2021; Available online: <https://ecsoc-25.sciforum.net>.

Abstract: The work seeks to identify molecules with inhibitory activity against the DNA gyrase of Gram-negative microorganisms resistant to fluoroquinolones. Previously designed compounds were used to study antimicrobial potential in silico. Molecular docking was performed with nine new ciprofloxacin analog molecules, optimized through the PM6/ZDO theory level, in GyrA wild type (WT) and mutant type (MT) of *C. jejuni*, *E. coli* (6RKU PDB ID), *N. gonorrhoeae*, *P. aeruginosa*, *S. enteritidis*, and *S. typhi*. The molecule with the highest affinity for GyrA was selected based on its binding free energy and inhibition constant. In addition, a retrospective docking was carried out, to guarantee the correct affinity of the ligand to the receptor at the defined binding site. The results show a molecule with greater affinity for GyrA in five microorganisms, showing a binding free energy of less than -7.0 kcal/mol, suggesting a good antibacterial activity in silico.

Keywords: molecular docking; fluoroquinolones; DNA gyrase; bacterial resistance



Citation: Coba-Males, M.A.; Santamaría-Aguirre, J.; Alcívar-León, C.D. In Silico Evaluation of New Fluoroquinolones as Possible Inhibitors of Bacterial Gyrases in Resistant Gram-Negative Pathogens.

Chem. Proc. **2022**, *8*, 43. <https://doi.org/10.3390/ecsoc-25-11753>

Academic Editor: Julio A. Seijas

Published: 14 November 2021

Publisher's Note: MDPI stays neutral with regard to jurisdictional claims in published maps and institutional affiliations.



Copyright: © 2022 by the authors. Licensee MDPI, Basel, Switzerland. This article is an open access article distributed under the terms and conditions of the Creative Commons Attribution (CC BY) license (<https://creativecommons.org/licenses/by/4.0/>).

1. Introduction

Fluoroquinolones are synthetic fluorinated antibiotics analogous to nalidixic acid that are born from a common basic chemical structure called 4-quinolone (4-oxo-1,4-dihydroquinoline), which consists of a bicyclic system with various substituents in its carbon atoms [1]. These compounds include a significant group of drugs with a major impact on antimicrobial chemotherapy, due to the discovery of nalidixic acid in 1962 by George Y. Leshner [2]. The introduction of norfloxacin as the first fluoroquinolone in 1980, obtained by the addition of a fluorine atom at position 6 of the quinolone pharmacophore group, was the beginning of the transcendental development of this new class of molecules [3]. They present a quick absorption in the gastrointestinal tract with high serum concentrations in 1–2 h, high bioavailability with large volume of distribution, low affinity for proteins, and plasma half-life of about 1.5–17 h [4].

The lack of effective antibiotics is an evident reality in all countries of the world due to the speed with which many microorganisms acquire resistance. In the last decade, antimicrobial resistance has become the greatest threat to global health facing humanity, putting at risk effective conventional antibiotic therapies against infectious diseases [5]. A report by PAHO (Pan American Health Organization) based on a study of bacterial resistance carried out in 15 Latin American countries during 2014–2016, indicates an average of more than 50% of non-sensitivity in gram-pathogens to fluoroquinolones in countries such as Brazil, Paraguay, Argentina, Chile, Colombia, and Peru [6].

Under those circumstances, the WHO (World Health Organization) published in 2017 the first list of priority antibiotic-resistant pathogens, with 12 species that represent a danger to human health, with the aim of encouraging research and development of new molecules [7], through the use of bioinformatic tools and computational models to find the most stable, specific and favorable manner for the interaction between a ligand and its receptor to take place [8]. Thus, molecular docking simulation has become a starting point for modeling the interaction between new molecules and their biological target [8], generating a positive impact on structure-based drug design (SBDD) [9].

Fluoroquinolones act by selectively inhibiting DNA gyrase or topoisomerase IV (key enzymes in the replication, transcription, and repair of bacterial DNA in gram-negative and gram-positive species, respectively) by preventing DNA supercoiling, action that takes place after intracellular antibiotic accumulation in the bacterial cytosol [10]. They bind to a region near tyrosine-122 (Tyr-122) in the N-terminal domain of the GyrA subunits of the DNA gyrase, to form a drug-enzyme-DNA ternary complex that blocks movement over the replication fork, transiently nullifying DNA, and mRNA synthesis [11].

DNA gyrase is a type II topoisomerase exclusive to prokaryotic organisms that is structurally composed of two subunits A (GyrA) and two subunits B (GyrB) with ATPase activity, both encoded by *gyrA* and *gyrB* genes respectively; the active enzyme is a heterotetrameric complex A₂B₂ [12], indispensable in DNA replication processes by reducing torsion stresses occurring in areas close to the replication fork at the time of unwinding of the circular DNA [13]. Subunit A is composed of an N-terminal domain (NTD) and a C-terminal domain (GyrA-CTD), being an important part of the enzyme for the recognition of some substrates, cell targeting, and interactions with other proteins; while subunit B is responsible for binding with ATP, its hydrolysis, and a support for DNA binding [14]. Some models based on observation and docking calculations have established the Quinolone Resistance Determining Region (QRDR) located in NTD of GyrA as the binding site for fluoroquinolones [15], because certain alterations of the DNA gyrase that confer resistance to fluoroquinolones reside in chromosomal mutations of genes encoding the target of the antibiotic [16].

This work seeks to investigate new fluoroquinolones derived from ciprofloxacin (CPX) that were designed by computational methods and evaluated by *molecular docking* in a previous study, where they showed high affinity and specificity against topoisomerase II of *Leishmania amazonensis* [17]. The aim was to predict the affinity of these compounds with the DNA gyrase wild type and mutant type of *Campylobacter jejuni*, *Escherichia coli*, *Neisseria gonorrhoeae*, *Pseudomonas aeruginosa*, *Salmonella enterica* serovar *enteritidis*, and *Salmonella enterica* serovar *typhi*, performing a *molecular docking* analysis to describe the interaction between these molecules and their pharmacological target and identify them as potential selective inhibitors of DNA gyrase. These docking results were validated through retrospective docking. In addition, it was determined whether there are structural differences between the DNA gyrase of the species in this study through multiple sequence alignment (MSA).

2. Materials and Methods

2.1. Preparation of Ligands

For each of the 9 molecules designed, its pKa and pH species distribution curve were calculated using the MarvinSketch 21.12.0 program and the predominant structure was selected at pH 7.0. Then, a previous energy optimization of each molecule was executed under the Universal Force-Field (UFF) in Avogadro 1.2.0, and an energy optimization and conformational analysis was performed through Gaussian 09W using a semi-empirical method with PM6/ZDO theory level, with the lowest energy conformer finally chosen to be considered in molecular docking.

2.2. Search for Protein Structures

The structure of the subunit A (GyrA) of the DNA gyrase WT was obtained from databases. GyrA from *Escherichia coli* was downloaded from RCSB Protein Data Bank as *E. coli* DNA Gyrase—DNA binding and cleavage domain in State 1 (6RKU PDB ID); GyrA WT de *Campylobacter jejuni* (GenBank ID: KRS63878.1), *Neisseria gonorrhoeae* (GenBank ID: GFL73998.1), *Pseudomonas aeruginosa* (GenBank ID: ARU38095.1), *Salmonella enterica* serovar *enteritidis* (GenBank ID: ANF19453.1), and *Salmonella enterica* serovar *typhi* (GenBank ID: ALG23216.1) were obtained from homology modeling on the SWISS-MODEL server starting from amino acid sequence downloaded from the National Center for Biotechnology Information (NCBI). We looked for the most suitable template for alignment with the target, and we selected a structure modeled with the best parameters of the estimated quality that were reported in each model. For GyrA MT structures in all microorganisms, the amino acid sequence was modified in the positions indicated in the literature [18–29], and homology modeling was performed in SWISS-MODEL. Finally, each protein structure was worked in UCSF Chimera 1.15. to maintain only one GyrA monomer.

2.3. Molecular Docking

This began with the preparation of the ligand and protein using AutoDockTools 1.5.6. For the structure of the protein, polar hydrogens and Kollman charges were added, and non-polar hydrogens were removed; for the ligand, all the hydrogens and Gasteiger charges were added, and non-polar hydrogens were removed. Next, the dimensions of the grid box were generated to cover the residues involved in the binding site of the enzyme, which includes all the amino acids within the QRDR, as established by the literature [12,15,30–35]. The parameters of the Lamarckian genetic algorithm were then selected and each coupling experiment with 10 different conformations was entrusted after a maximum of 2,500,000 energy evaluations. Then, virtual screening was performed using the Raccoon 1.0 extension, where all ligands were loaded with the protein, as well as the grid configuration files (gpf format) and the docking (dpf format). Finally, the program was executed with AutoDock 4.2.6 to obtain the docking results for analysis by AutoDockTools 1.5.6, where the values of free binding energy, inhibition constant, total intermolecular energy, and electrostatic energy were tabulated for each conformation of the 9 molecules in the docking with wild type and mutant type enzymes for the 6 microorganisms. Then, a treatment to classify via scoring system was carried out, the best molecules having high affinity for GyrA. The lowest quintile was calculated in each parameter and from this a threshold value was calculated with which a score of “1” or “5” was assigned to each conformation, according to some criteria in order of priority of their biological relevance (Table S1). Subsequently, the total score was obtained by multiplying each result, with 625 being the highest value to be reached in a conformation of a molecule. Likewise, we calculated the average of the total score for each molecule considering its 10 conformations. Finally, interactions with GyrA residues were analyzed by Discovery Studio 2021.

2.4. Multiple Sequence Alignment

All GyrA WT structures were loaded to the UCSF Chimera 1.15 program and a MatchMaker was made for a structural superposition of proteins, selecting the GyrA WT structure of *E. coli* as a reference for this process. Finally, an alignment was made from the initially generated overlap, and the alignment of sequences in the QRDR was visualized. The same procedure was performed for GyrA MT structures.

2.5. Retrospective Docking

Active and inactive compounds against GyrA were identified based on bioassays published in the PubChem database [36]. The compounds were treated under the same procedure indicated in 2.1. Preparation of Ligands to identify the minimum energy structure. Subsequently, a blind docking was carried out with the GyrA MT of *E. coli*, *P. aeruginosa*, and *S. enterica* serovar *typhi*, preparing the ligand and the protein as detailed in 2.3. Molecular

Docking. The grid box was configured to cover the protein in its entirety, and then the parameters of the Lamarckian genetic algorithm were configured so that 15 different conformations were derived from each docking after a maximum of 2,500,000 energy evaluations. Then, the virtual screening was realized using the extension of Raccoon 1.0. in the same way as the molecular docking. Finally, the results of the blind docking were analyzed through UCSF Chimera 1.15, where the binding site where there were the greatest number of conformations was observed. In addition, these results were analyzed by AutoDockTools 1.5.6 visualizing the positions in which these ligands were in relation to the grid box used in the molecular docking with the new fluoroquinolones.

3. Results and Discussion

The study evaluated nine new fluoroquinolones as possible inhibitors of DNA gyrase in resistant gram-negative pathogens using computational methods.

3.1. General Characteristics of the Ligands

The pKa values and the total energy of the minimum energy conformer for the new fluoroquinolone molecules analogous to ciprofloxacin used in this study are shown in Table 1. Permeability studies in artificial membranes have shown that the capacity and manner in which fluoroquinolones penetrate the cell membrane is a complex process that depends on physical and chemical factors [37]; since these molecules mainly cross the membranes by passive transport at physiological pH, it is important to know their ionization state as a result of their amphoteric nature by the presence of ionizable groups in their structure.

Table 1. Total energy and pKa of the new fluoroquinolones.

Molecule	pKa	Total Energy (kcal/mol)
1	5.42; 6.96	−77.204
2	5.20; 6.94	−94.002
3	5.22; 10.01	−81.015
4	5.13; 9.62	−61.277
5	5.22; 10.01	−106.831
6	5.41; 14.76	−99.272
7	5.17; 10.00	−74.914
8	5.80; 14.77	−97.200
9	5.45; 9.56	−32.860

Depending on the pH of the medium, it is possible to find four micro species at different concentrations: a basic ionic form (Q^-), an acidic ionic form (H_2Q^+), a neutral form (HQ), and a hybrid ion or zwitterion (HQ^\pm). The pKa values shown in Table 1 are mainly considered for the two relevant ionizable groups at position 3 and on the side chain at position 7 of the fluoroquinolone structure; in addition, there are other very weak ionizable groups with no greater percentage in their concentration, so these values have been disregarded. It can be observed that for the 9 molecules the pKa₁ corresponding to the dissociation of carboxylic acid on C₃ ranges from 5.13 to 5.80; while the pKa₂ corresponding to the dissociation of nitrogen on the side chain on C₇ takes values from 6.94 to 14.77. According to the pKa values and the microspecies distribution curve for each molecule (Figure S1), the predominant form at pH 7.0 for molecules 1, 2, 5, 6, and 8 was the basic ionic form; while for molecules 3, 4, 7, and 9, the zwitterionic form prevailed. The latter has a significant dipole that at physiological pH usually predominates over the neutral species and additionally expresses a better antibacterial activity, which has led some studies to consider the possibility that these species can diffuse through the membrane by passive transport to some extent, even in molecules of high molecular weight [38].

However, in minimum energy structures (Figure S2) of molecules 3 and 7 it was observed that the most stable conformation shown corresponds to the neutral form of

fluoroquinolone reaching energy values of -81.015 and -74.914 kcal/mol, respectively. This is probably due to the spatial arrangement of their atoms, especially in the protonated nitrogen of the side chain and the carboxylate of the 3rd position, where, by difference in electronegativity oxygen, it can recapture the hydrogen again to provide more stability to the modeling molecule in the gas state. The authors claim that the crossing of these molecules through the lipid bilayer usually occurs only with non-ionized forms [38].

3.2. Alignment of GyrA Protein Structures

The multiple alignment of sequences for the structures of the GyrA in the six microorganisms allows us to show the structural differences that may influence the biological function of the protein. The sequences for GyrA WT and MT were aligned based on the *E. coli* GyrA sequence (6RKU PDB ID) as a reference, and the sequence of this protein was determined by cryo-electron microscopy [39].

3.2.1. Identity between GyrA WT Structures

The identity percentages obtained from the multiple alignment of sequences in the GyrA WT of the six Gram-negative microorganisms exceed 50% in all comparisons, indicating a structural homology between them (Figure 1) since two proteins are considered as homologous when they reach a percentage greater than or equal to 25% [40]. This identity is commonly used to identify certain conserved regions of interest that allow location of the active site of an enzyme in species that have some evolutionary relationship [41]. Among the results, it is interesting to note the value reached between *E. coli* and the two sero-varieties of *S. enterica*, *enteritidis* and *typhi*, which were 83.46% and 95.16%, respectively (Table S2). This would indicate a structural similarity of the DNA gyrase, something that is also corroborated with some genetic and molecular studies in these species that suggest a great genetic identity, as these mention the divergence of both genera from a common ancestor about 100 million years ago; in addition it is known that about 50% of the virulent genes of *Salmonella* are also present in *E. coli*, some of these responsible for synthesizing proteins responsible for repairing damage to the DNA of the microorganism [42].

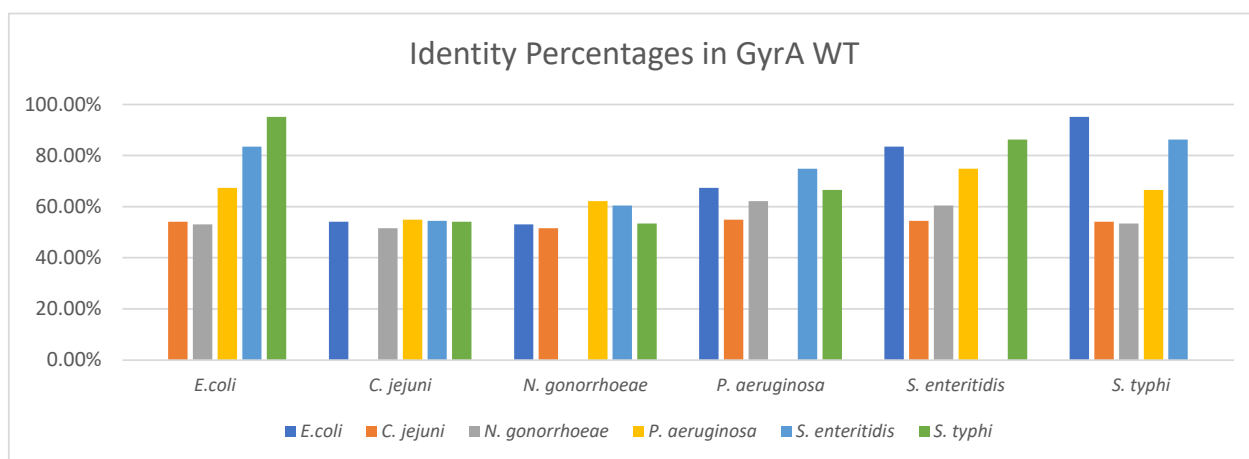


Figure 1. The identity percentages achieved for the GyrA WT between each of the species of microorganisms in relation to the GyrA WT of *E. coli*.

The identity percentages were obtained from the results provided by the multiple alignment of the amino acid sequence that codes for the subunit A in DNA gyrase by the *gyrA* gene (Figure S3), since the primary structure determines the folding of the protein, which is related to its three-dimensional structure [43].

The alignment on QRDR was analyzed, since it is the site where drug-receptor interactions take place; except for species such as *C. jejuni* and *N. gonorrhoeae*, QRDR in the other four microorganisms included around 67–106 residues, which shows a high conservation

of amino acids, which also suggests a high affinity of the same molecule for the gyrase of different microorganisms. While for *C. jejuni* and *N. gonorrhoeae*, changes of some residues on their corresponding QRDR regions are evident, differing slightly from the amino acids of the other sequences, which is reflected in an identity that does not exceed 55%.

3.2.2. Identity between GyrA MT Structures

The results shown for GyrA MT in the six microorganisms (Figure 2) do not differ significantly (Table S3) to those of GyrA WT. These enzymes have mutations in two or three amino acids, which give the microorganism the property of acquiring resistance against fluoroquinolones within the QRDR, which usually occur in the same position but with a different residue.

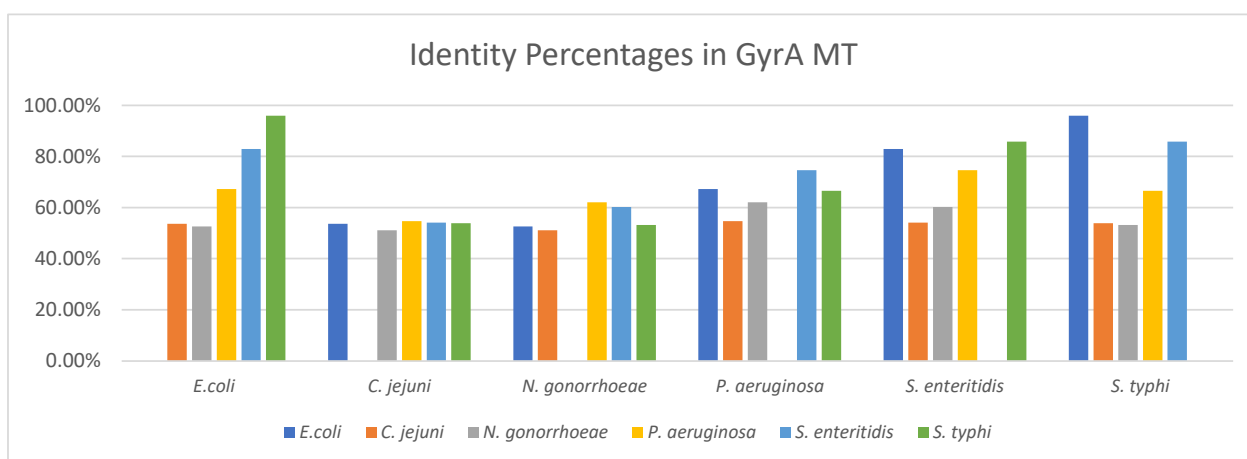


Figure 2. The identity percentages achieved for the GyrA MT between each of the species of microorganisms in relation to the GyrA MT of *E. coli*.

The identity percentages were obtained from the results provided by the multiple alignment of the amino acid sequence for GyrA MT (Figure S4). Although the alignment carried out considers the mutations in residues within the QRDR region, there are changes in the amino acids that maintain similar physico-chemical characteristics and allow a substitution between them [44]. This means that despite showing a different sequence, proteins do not differ notably in their structure, therefore they maintain their biological function and the same three-dimensional folding.

3.3. Molecular Docking

All results obtained from molecular docking performed at pH 7.0 for the nine molecules included in the docking with wild type and mutant type enzymes are fully shown in the Supplementary Material (Tables S5–S28).

3.3.1. Molecular Docking Results in GyrA MT of *Campylobacter jejuni*

Table 2 shows the statistical treatment carried out in subunit A of the DNA gyrase MT in *Campylobacter jejuni*, where for each parameter, the calculation of the lowest quintile was made from the quotient between the difference between the maximum with the lowest value obtained from the whole data set and divided by five. From this result, the threshold value was obtained for the difference between the minimum value and the calculated quintile; the threshold value was used to establish the score that subsequently allowed identification of a group of better molecules.

Molecule 7 in its conformation 3 was the best molecule with a high score in the docking with the GyrA MT of *C. jejuni*, which had the lowest binding free energy, -7.14 kcal/mol, and jointly obtained the lowest inhibition constant, of 5.82 μ M, compared to the other molecules (Table S4), even better than ciprofloxacin which reached values of -6.32 kcal/mol

and 23.29 μM , respectively, for binding energy and inhibition constant. Therefore, it is evident that molecule 7 has a greater affinity for its receptor in a spontaneous process allowing the binding of the drug to the protein with a suitable orientation [45] and requiring low concentrations, suggesting a good efficacy of the antagonist drug to inhibit the activity of bacterial gyrase [46].

Table 2. Statistical treatment for docking in GyrA MT of *C. jejuni*.

	Binding Free Energy (kcal/mol)	Inhibition Constant (μM)	Total Intermolecular Energy (kcal/mol)	Electrostatic Energy (kcal/mol)
Min.	−7.14	5.82	−8.93	−2.2
Max.	−5.06	194.14	−6.26	−0.32
R	2.08	188.32	2.67	1.88
R/5	0.416	37.664	0.534	0.376
Threshold Value	−6.724	43.484	−8.396	−1.824

Min.: the minimum value obtained among all the data. Max.: the maximum value obtained among all the data. R: difference between the maximum value and the minimum value. R/5: lowest quintile. Threshold Value: min.−(R/5).

3.3.2. Summary of Molecular Docking Results

Table 3 summarizes the best values of the parameters and shows molecule 7 to have the highest affinity against GyrA of each microorganism. Molecule 7 showed high affinity with topoisomerase II in *Leishmania amazonensis* and with the DNA gyrase of *Salmonella*, and low affinity with human α and β topoisomerases, under an in-silico study that also indicates compliance with the properties of this new molecule against Lipinski's rule of five [17]. These favorable features suggest this compound for further studies at experimental level.

Table 3. Fluoroquinolone molecules with higher affinity for GyrA.

Molecule	Microorganism	Binding Free Energy (kcal/mol)	Inhibition Constant (μM)	Total Intermolecular Energy (kcal/mol)	Electrostatic Energy (kcal/mol)
7	<i>C. jejuni</i> MT	−7.14	5.82	−8.93	−1.22
CPX		−6.32	23.29	−7.22	−0.84
7	<i>C. jejuni</i> WT	−7.64	2.51	−9.43	−0.83
CPX		−6.2	28.52	−7.1	−1.64
7	<i>E. coli</i> MT	−7.45	3.44	−9.24	−1.3
CPX		−6.46	18.53	−7.35	−1.09
7	<i>E. coli</i> WT	−7.44	3.54	−9.23	−1.24
CPX		−6.29	24.65	−7.18	−0.94
3	<i>N. gonorrhoeae</i> MT	−6.81	10.21	−8.3	−2.53
CPX		−6.52	16.51	−7.42	−1.53
7	<i>N. gonorrhoeae</i> WT	−7.11	6.14	−8.9	−1.74
CPX		−6.15	31.21	−7.04	−1.86
7	<i>P. aeruginosa</i> MT	−8.13	1.1	−9.92	−1.51
CPX		−6.38	21.22	−7.27	−1.54
7	<i>P. aeruginosa</i> WT	−7.95	1.48	−9.74	−1.43
CPX		−6.5	17.13	−7.4	−1.46
5	<i>S. enteritidis</i> MT	−7.91	1.58	−9.11	−0.99
CPX		−6.49	17.56	−7.38	−0.93
5	<i>S. enteritidis</i> WT	−7.75	2.1	−8.94	−0.87
CPX		−6.43	19.44	−7.32	−1.3
7	<i>S. typhi</i> MT	−7.38	3.92	−9.17	−1.2
CPX		−6.28	24.96	−7.17	−0.93
7	<i>S. typhi</i> WT	−7.38	3.89	−9.17	−1.27
CPX		−6.31	23.84	−7.2	−0.99

3.3.3. Results of Interactions in Molecular Docking

The residues involved in the interaction with the best conformation of the molecule are highly variable from species to species. In this sense, among the enzymes of the same bacterium, there are similarities, and they offer an overview of their influence on the stable formation of the drug-protein complex; although within QRDR, it is possible to establish similarities between all microorganisms (Table S29).

For *E. coli* and *S. typhi*, two enterobacteria under molecular and genetic criteria to some extent similar, share interactions in residues Pro95, Met101, Asp104, Gly105, through hydrogen bridges at an average distance between 2.0 and 3.0 Å, which occurs with the carboxyl group of position 3, the carbonyl group in C₄, and the amino group of the side chain on C₇ (Figure 3); this type of interaction is strong in the binding of fluoroquinolone to the enzyme, because amino acids are near the active site of the protein [47].

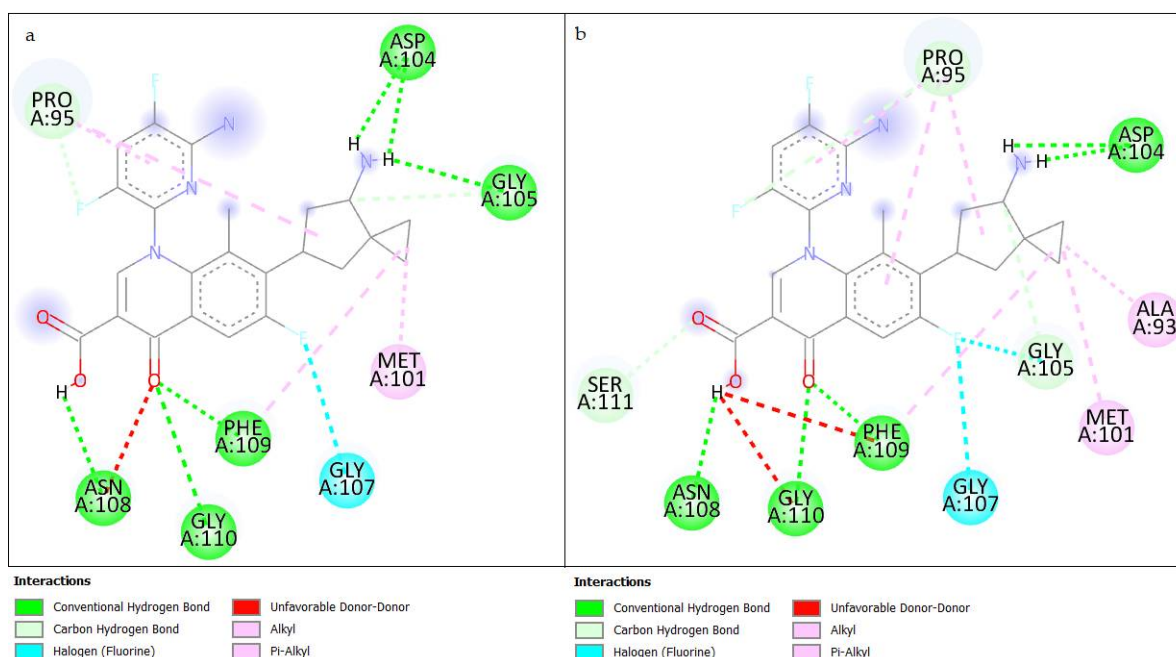


Figure 3. Interactions of molecule 7 with residues of GyrA MT from (a) *E. coli* and (b) *S. typhi*, obtained after molecular docking through the Discovery Studio program.

Among the residues involved in the interaction of *P. aeruginosa* and *S. enteritidis*, Arg91 (Figure S5), a non-covalent bond with an electrostatic nature, plays an important role in the rigidity and stability of a ligand-receptor complex [48].

On the other hand, there are no similarities in the interactions registered for *C. jejuni* and *N. gonorrhoeae* (Figure S6), probably because the position of their QRDR differs in both cases, occurring between residues 69–120 and 55–110, respectively, which generates different docking positions for each case. Although the appearance of interactions by hydrogen and hydrophobic bridges is highlighted in both species, the latter are very weak and not significant due to the presence of hydrophobic residues such as Val and Tyr [49]. However, its presence is justified by the aromaticity of the fluoroquinolone molecule.

Therefore, the mutations induced in those residues reported by the literature as the main ones involved in the resistance to fluoroquinolones did not produce a significant change in the interaction with these new molecules, suggesting an important performance of these compounds against resistant pathogens.

3.4. Retrospective Docking

In view of the fact that there is no software capable of accurately predicting the mode of binding between a molecule and its receptor [8], and in order to ensure a good agreement

on the docking generated by the algorithm used in AutoDock 4.2.6 between the ligands and their protein target, a retrospective docking was carried out from a library of ligands and decoy molecules, observing the binding sites in which the docking of the molecules with activity takes place primarily in front of the protein [50].

We worked with a comparative methodology, using active and inactive molecules (Figure S7) in the GyrA MT of *E. coli*, *P. aeruginosa*, and *S. typhi*. Thus, based on the capacity of the software, it will be possible to differentiate the active molecules from those that do not bind to the active site of the protein [8].

Retrospective Docking in GyrA MT of *E. coli*

Figure 4 shows the docking for some conformations of each of the four fluoroquinolone molecules that were used as ligands, with activity against the DNA gyrase; the selection of conformations was carried out after observational analysis of a total of 15 different modes in which the ligand binds to the receptor. Priority was given to the site in which there is a greater number of conformations for the same molecule. For Moxifloxacin, a conformation away from the common site where molecules such as Ofloxacin, Delafloxacin, and Gatifloxacin coincided was observed, but from the three-dimensional view it was evident that this molecule was positioned in a back plane close to this binding site; therefore, this coupling was also considered.

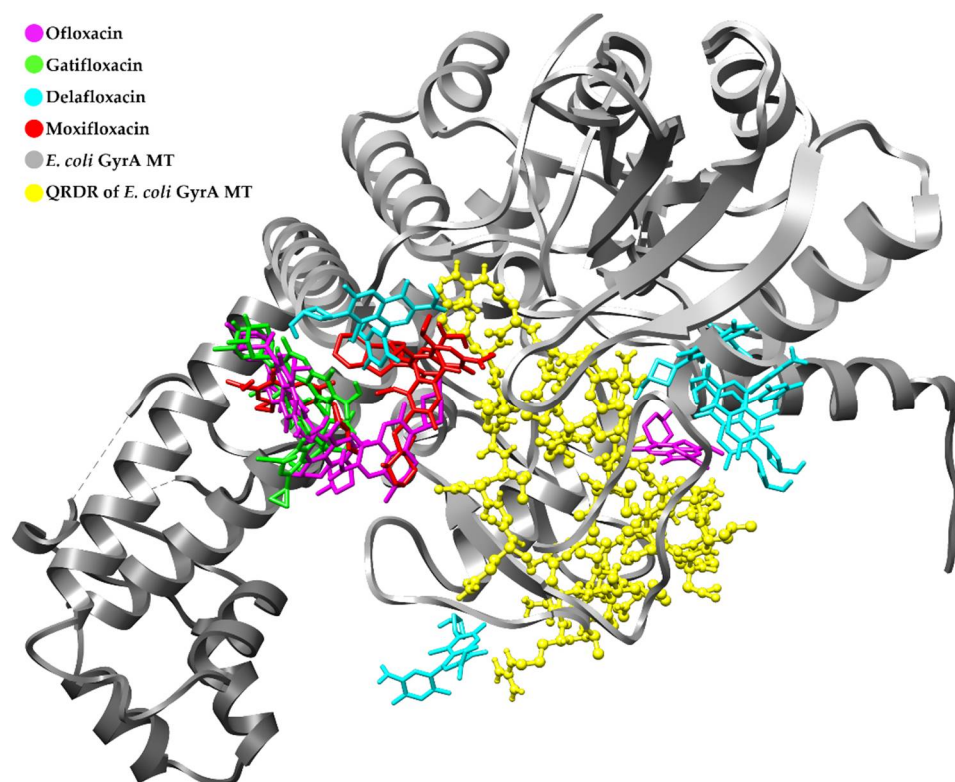


Figure 4. Image obtained using the UCSF Chimera program showing the blind docking results with some conformations for the active molecules, each one represented in stick model by a characteristic color; docked in GyrA MT of *E. coli* in the ribbon diagram and ball & stick model in gray as target, QRDR is highlighting in yellow.

When analyzing the results of the blind docking obtained with the four fluoroquinolones, it was observed that most of the docking occurs in an area too close to the region covered by the grid defined as the binding site of the new molecules with which we worked during this investigation (Table S8). In some cases, conformations within the grid were evident, with the possibility of interactions with residues from the QRDR region, a binding site characteristic of fluoroquinolones.

Figure 5 shows the docking of some conformations for four molecules that do not show pharmacological potential against the DNA gyrase; the best conformations were selected in the same way that was considered for the active molecules in the previous case. Here, we could observe a diverse affinity of inactive molecules by different sites throughout the structure of the protein.

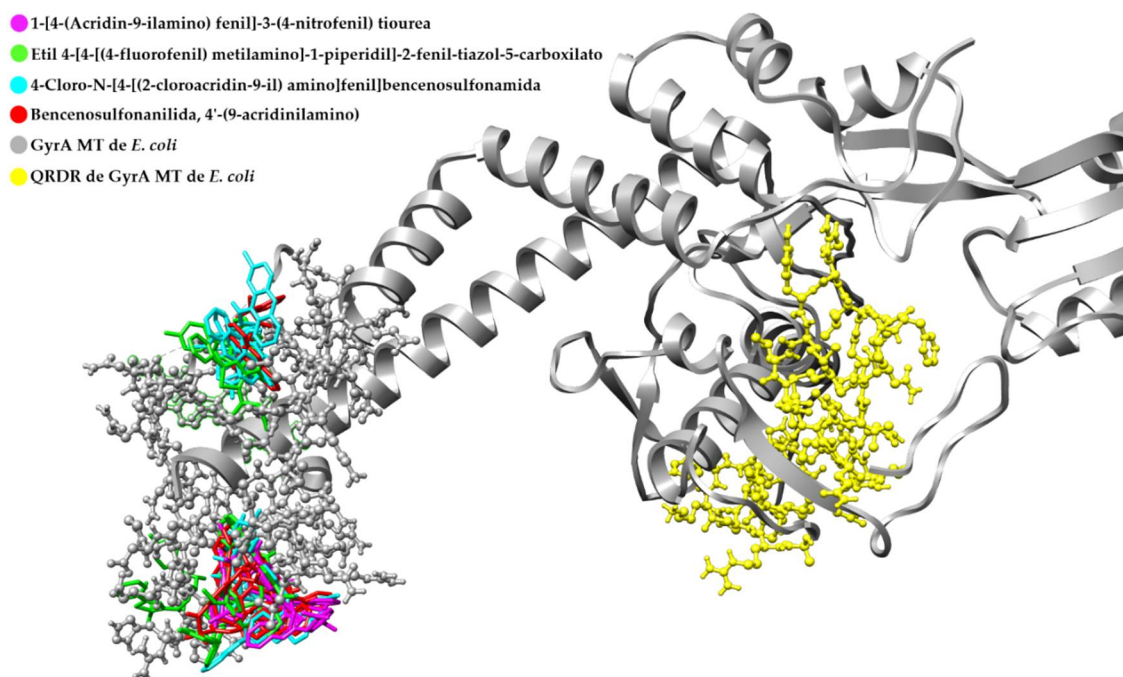


Figure 5. Image obtained using the UCSF Chimera program showing the blind docking results with some conformations for the inactive molecules, each one represented in stick model by a characteristic color; docked in GyrA MT of *E. coli* in the ribbon diagram and ball & stick model in gray as target, QRDR is highlighting in yellow.

When analyzing the positions of the different couplings generated in the *blind docking* in relation to the position covered by the grid, it was observed that several conformations of the inactive molecules are far from the QRDR (Figure S9). This explains the inactivity of these compounds against GyrA, as has been mentioned in bioassays made with these molecules, where synthetic molecules of heteroaromatic tricyclic acrylic bound to a *p*-phenylenediamine group, obtained through the modification of a hybrid molecule of quinoline-aminopiperidine, inhibited with high specificity the DNA gyrase of *M. tuberculosis*, but showed no activity against the DNA gyrase of *S. aureus*, *E. coli*, and *P. aeruginosa* during DNA supercoiling assays [36].

The validation of the GyrA MT of *P. aeruginosa* (Figures S10–S13) showed that the conformations of the active compounds are close to each other and included within the grid, while in the inactive molecules, most of their conformations are attached to one end of the protein. Although the presence of few structures near the grid region was evident, this was not a predominant binding site that suggests the affinity of these compounds.

On the other hand, the images obtained for the validation of GyrA MT in *S. typhi* (Figures S14–S17) showed a coupling in a region quite close to the grid for most conformations in fluoroquinolones, while the inactive compounds were attached to one end of the protein structure.

Considering the results, the existence of a degree of affinity between the new molecules and the GyrA was established with reliable molecular docking results; whereas after retrospective docking, it was observed that compounds with inhibitory activity on the DNA gyrase reported by the literature were coupled over a very close area or within the QRDR, a place that was defined as the binding site of the nine designed molecules,

and where the docking of most of their conformations occurred. Therefore, based on the experimental molecular docking results initially obtained, it is assumed that molecule 7 should have a good probability of being active against the GyrA; this compound has demonstrated a high affinity for its receptor in terms of free binding energy, which would lead it to be a candidate for further experimental studies.

4. Conclusions

The results of molecular docking point to molecule 7 as having the largest affinity against the subunit A of the DNA gyrase wild type and mutant type of *Campylobacter jejuni*, *Escherichia coli*, *Pseudomonas aeruginosa*, and *Salmonella enterica* serovar *typhi*, suggesting it as a possible bacterial gyrase inhibitor in resistant gram-negative pathogens, by showing better affinity parameters with respect to its analog ciprofloxacin. Retrospective docking ensures that the affinity shown by new molecules to GyrA has a good degree of reliability, as several conformations of active compounds bind to an area very close to QRDR, defined as the preferential binding site in experimental docking performed with new fluoroquinolones. In vitro studies are needed to confirm the effectiveness of these compounds.

Supplementary Materials: The following supporting information can be downloaded at: <https://www.mdpi.com/article/10.3390/ecsoc-25-11753/s1>: Table S1. Biologically relevant criteria used in the scoring system to classify molecules with greater affinity for GyrA, Table S2. Identity percentage between structures of GyrA WT, Table S3. Identity percentage between structures of GyrA MT, Table S4. Molecules with higher affinity for GyrA MT of *C. jejuni*, Table S5. Statistical treatment for docking in gyrA WT of *C. jejuni*, Table S6. Molecules with higher affinity for GyrA WT of *C. jejuni*, Table S7. Statistical treatment for docking in gyrA MT of *E. coli*, Table S8. Molecules with higher affinity for GyrA MT of *E. coli*, Table S9. Statistical treatment for docking in gyrA WT of *E. coli*, Table S10. Molecules with higher affinity for GyrA WT of *E. coli*, Table S11. Statistical treatment for docking in gyrA MT of *N. gonorrhoeae*, Table S12. Molecules with higher affinity for GyrA MT of *N. gonorrhoeae*, Table S13. Statistical treatment for docking in gyrA WT of *N. gonorrhoeae*, Table S14. Molecules with higher affinity for GyrA WT of *N. gonorrhoeae*, Table S15. Statistical treatment for docking in gyrA MT of *P. aeruginosa*, Table S16. Molecules with higher affinity for GyrA MT of *P. aeruginosa*, Table S17. Statistical treatment for docking in gyrA WT of *P. aeruginosa*, Table S18. Molecules with higher affinity for GyrA WT of *P. aeruginosa*, Table S19. Statistical treatment for docking in gyrA MT of *S. enteritidis*, Table S20. Molecules with higher affinity for GyrA MT of *S. enteritidis*, Table S21. Statistical treatment for docking in gyrA WT of *S. enteritidis*, Table S22. Molecules with higher affinity for GyrA WT of *S. enteritidis*, Table S23. Statistical treatment for docking in gyrA MT of *S. typhi*, Table S24. Molecules with higher affinity for GyrA MT of *S. typhi*, Table S25. Statistical treatment for docking in gyrA WT of *S. typhi*, Table S26. Molecules with higher affinity for GyrA WT of *S. typhi*, Table S27. Docking results in ciprofloxacin with higher affinity for GyrA, Table S28. Average scores for new molecules in molecular docking with GyrA, Table S29. Molecular docking interactions with GyrA residues, Figure S1. Species distribution curve as a function of pH for the designed fluoroquinolones, Figure S2. Low-energy 3D structures of designed fluoroquinolones, Figure S3. Multiple sequences alignment on the QRDR for GyrA WT obtained through the UCSF Chimera program, Figure S4. Multiple sequences alignment on the QRDR for GyrA MT obtained through the UCSF Chimera program, Figure S5. Interactions with GyrA residues MT from (a) molecule 7 in *P. aeruginosa*, and (b) molecule 5 in *S. typhi*; obtained after molecular coupling through the Discovery Studio program, Figure S6. Interactions with GyrA residues MT from (a) molecule 7 in *C. jejuni*, and (b) molecule 3 in *N. gonorrhoeae*; obtained after molecular coupling through the Discovery Studio, Figure S7. Structures of active and inactive compounds used for retrospective docking, Figure S8. Blind docking result with active ligands in GyrA of *E. coli*, Figure S9. Blind docking result with inactive ligands in GyrA of *E. coli*, Figure S10. Molecular docking of the active ligands against the GyrA of *P. aeruginosa*, Figure S11. Molecular docking of the inactive ligands against the GyrA of *P. aeruginosa*, Figure S12. Blind docking result with active ligands in GyrA of *P. aeruginosa*, Figure S13. Blind docking result with inactive ligands in GyrA of *P. aeruginosa*, Figure S14. Molecular docking of the active ligands against the GyrA of *S. typhi*, Figure S15. Molecular docking of the inactive ligands against the GyrA of *S. typhi*, Figure S16. Blind docking result with active ligands in GyrA of *S. typhi*, Figure S17. Blind docking result with inactive ligands in GyrA of *S. typhi*. References [51–53] are cited in the Supplementary Materials.

Author Contributions: Conceptualization and molecules design, J.S.-A.; methodology, J.S.-A. and M.A.C.-M.; formal analysis, M.A.C.-M.; investigation, M.A.C.-M.; project administration, J.S.-A.; writing—original draft preparation, M.A.C.-M.; writing—review and editing, J.S.-A. and C.D.A.-L. All authors have read and agreed to the published version of the manuscript.

Funding: This research received no external funding.

Institutional Review Board Statement: Not applicable.

Informed Consent Statement: Not applicable.

Data Availability Statement: The data presented in this study will be openly available online.

Acknowledgments: We are grateful to ARES program since this study is part of the Nanofloxacin: Leishmanicidal Activity project. We thank Martín J. Lavecchia for providing some useful recommendations and comments to improve the technical quality and results of this manuscript. Christian D. Alcívar León is thankful for the financial support from the Central University of Ecuador (Grant, DI-CON-2019-007), Faculty of Chemical Sciences.

Conflicts of Interest: The authors declare no conflict of interest.

References

1. Brar, R.K.; Jyoti, U.; Patil, R.K.; Patil, H.C. Fluoroquinolone antibiotics: An overview. *Adesh. Univ. J. Med. Sci. Res.* **2020**, *2*, 26–30. [CrossRef]
2. Mohammed, H.H.H.; Abu-Rahma, G.E.-D.A.A.; Abbas, S.H.; Abdelhafez, E.-S.M.N. Current Trends and Future Directions of Fluoroquinolones. *Curr. Med. Chem.* **2019**, *26*, 3132–3149. [CrossRef] [PubMed]
3. Higgins, P.G.; Fluit, A.C.; Schmitz, F.-J. Fluoroquinolones: Structure and Target Sites. *Curr. Drug Targets* **2003**, *4*, 181–190. [CrossRef] [PubMed]
4. Arés, F.; Martínez de la Ossa, R.; Alfayate, S. Quinolonas en Pediatría. *Rev. Pediatría Atención Primaria* **2017**, *19*, e83–e92.
5. Resistencia a los Antibióticos. Available online: <http://www.who.int/es/news-room/fact-sheets/detail/resistencia-a-los-antibióticos> (accessed on 15 July 2021).
6. Resistencia a los Antimicrobianos. Available online: <https://www.paho.org/es/documentos/magnitud-tendencias-resistencia-antimicrobianos-latinoamerica-relavra-2014-2015-2016> (accessed on 15 July 2021).
7. La OMS Publica la Lista de las Bacterias para las que se Necesitan Urgentemente Nuevos Antibióticos. Available online: <https://www.who.int/es/news/item/27-02-2017-who-publishes-list-of-bacteria-for-which-new-antibiotics-are-urgently-needed> (accessed on 15 July 2021).
8. Ballón, W.; Grados, R. Acomplamiento molecular: Criterios prácticos para la selección de ligandos biológicamente activos e identificación de nuevos blancos terapéuticos. *Rev. Con-Cienc.* **2019**, *7*, 55–72.
9. De Vivo, M.; Masetti, M.; Bottegoni, G.; Cavalli, A. Role of Molecular Dynamics and Related Methods in Drug Discovery. *J. Med. Chem.* **2016**, *59*, 4035–4061. [CrossRef]
10. Serra, H.A. Quinolonas. *Separata* **2008**, *16*, 1–9.
11. Bakken, J.S. The Fluoroquinolones: How Long Will Their Utility Last? *Scand J. Infect. Dis.* **2004**, *36*, 85–92. [CrossRef]
12. Heddle, J.G.; Barnard, F.M.; Wentzell, L.M.; Maxwell, A. The Interaction of Drugs with DNA Gyrase: A Model for the Molecular Basis of Quinolone Action. *Nucleosides Nucleotides Nucleic Acids* **2000**, *19*, 1249–1264. [CrossRef]
13. Pierce, B.A. *Génética. un Enfoque Conceptual*, 3rd ed.; Editorial Médica Panamericana: Madrid, Spain, 2009; p. 730.
14. Khan, T.; Sankhe, K.; Suvarna, V.; Sherje, A.; Patel, K.; Dravyakar, B. DNA gyrase inhibitors: Progress and synthesis of potent compounds as antibacterial agents. *Biomed. Pharm.* **2018**, *103*, 923–938. [CrossRef]
15. Madurga, S.; Sánchez, J.; Belda, I.; Vila, J.; Giralt, E. Mechanism of Binding of Fluoroquinolones to the Quinolone Resistance-Determining Region of DNA Gyrase: Towards an Understanding of the Molecular Basis of Quinolone Resistance. *ChemBioChem* **2008**, *9*, 2081–2086. [CrossRef] [PubMed]
16. Rodríguez, J.M. Mecanismos de resistencia a quinolonas mediada por plásmidos. *Enferm. Infecc. Microbiol. Clin.* **2005**, *23*, 25–31. [CrossRef] [PubMed]
17. Jacho, M. Métodos Computacionales para el Diseño de Fluoroquinolonas con Alta Afinidad por Topoisomerasa II de Leishmania. Bachelor's Thesis, Universidad Central del Ecuador, Quito, Ecuador, 2020.
18. Varughese, L.R.; Rajpoot, M.; Goyal, S.; Mehra, R.; Chhokar, V.; Beniwal, V. Analytical profiling of mutations in quinolone resistance determining region of gyrA gene among UPEC. *PLoS ONE* **2018**, *13*, e0190729. [CrossRef] [PubMed]
19. Zhao, L.; Wang, S.; Li, X.; He, X.; Jian, L. Development of in vitro resistance to fluoroquinolones in *Pseudomonas aeruginosa*. *Antimicrob. Resist. Infect. Control.* **2020**, *9*, 1–8. [CrossRef] [PubMed]
20. Nouri, R.; Ahangarzadeh, M.; Hasani, A.; Aghazadeh, M.; Asgharzadeh, M. The role of gyrA and parC mutations in fluoroquinolones-resistant *Pseudomonas aeruginosa* isolates from Iran. *Braz. J. Microbiol* **2016**, *47*, 925–930. [CrossRef]

21. Hakanen, A.; Jalava, J.; Kotilainen, P.; Jousimies-Somer, H.; Siitonen, A.; Huovinen, P. gyrA Polymorphism in *Campylobacter jejuni*: Detection of gyrA Mutations in 162 C. jejuni Isolates by Single-Strand Conformation Polymorphism and DNA Sequencing. *Antimicrob. Agents Chemother.* **2002**, *46*, 2644–2647. [CrossRef]
22. Paravisi, M.; Laviniki, V.; Bassani, J.; KKunert Filho, H.; Carvalho, D.; Wilsmann, D.; Borges, K.; Furian, T.; Salle, C.; Moraes, H.; et al. Antimicrobial Resistance in *Campylobacter jejuni* Isolated from Brazilian Poultry Slaughterhouses. *Braz. J. Poult. Sci.* **2020**, *22*, 1–9. [CrossRef]
23. Da Silva, B.; Medeiros, V.; Barbosa, A.V.; Silva, W.; Faccini, F.; Lima da Costa, D.; Clementino, M.; Cosendey, M. Detection of fluoroquinolone resistance by mutation in gyrA gene of *Campylobacter* spp. isolates from broiler and laying (*Gallus gallus domesticus*) hens, from Rio de Janeiro State, Brazil. *Ciencia Rural* **2015**, *45*, 2013–2018. [CrossRef]
24. Kivata, M.W.; Mbuchi, M.; Eyase, F.L.; Bulimo, W.D.; Kyanya, C.K.; Oundo, V.; Muriithi, S.W.; Andagalu, B.; Mbinda, W.M.; Soge, O.O.; et al. GyrA and parC mutations in fluoroquinolone-resistant *Neisseria gonorrhoeae* isolates from Kenya. *BMC Microbiol.* **2019**, *19*, 1–9. [CrossRef]
25. Kumar, M.; Dahiya, S.; Sharma, P.; Sharma, S.; Singh, T.P.; Kapil, A.; Kaur, P. Structure Based In Silico Analysis of Quinolone Resistance in Clinical Isolates of *Salmonella* Typhi from India. *PLoS ONE* **2015**, *10*, e0126560. [CrossRef]
26. Britto, C.D.; Dyson, Z.A.; Mathias, S.; Bosco, A.; Dougan, G.; Jose, S.; Nagaraj, S.; Holt, K.E.; Pollard, A.J. Persistent circulation of a fluoroquinolone-resistant *Salmonella enterica* Typhi clone in the Indian subcontinent. *J. Antimicrob. Chemother.* **2020**, *75*, 337–341. [CrossRef] [PubMed]
27. Vidovic, S.; An, R.; Rendahl, A. Molecular and physiological characterization of fluoroquinolone-highly resistant salmonella enteritidis strains. *Front. Microbiol.* **2019**, *10*, 1–12. [CrossRef] [PubMed]
28. Ma, Y.; Li, M.; Xu, X.; Fu, Y.; Xiong, Z.; Zhang, L.; Qu, X.; Zhang, H.; Wei, Y.; Zhan, Z.; et al. High-levels of resistance to quinolone and cephalosporin antibiotics in MDR-ACSSuT *Salmonella enterica* serovar Enteritidis mainly isolated from patients and foods in Shanghai, China. *Int. J. Food Microbiol.* **2018**, *286*, 190–196. [CrossRef] [PubMed]
29. Kuang, D.; Zhang, J.; Xu, X.; Shi, W.; Chen, S.; Yang, X.; Su, X.; Shi, X.; Meng, J. Emerging high-level ciprofloxacin resistance and molecular basis of resistance in *Salmonella enterica* from humans, food and animals. *Int. J. Food Microbiol.* **2018**, *280*, 1–9. [CrossRef]
30. Davila, C.; Llach, L.; Salgado-Moran, G.; Ramirez-Tagle, R. Docking studies on novel analogs of quinolones against DNA gyrase of *Escherichia coli*. *J. Pharm. Pharm. Res.* **2018**, *6*, 386–391.
31. Pacheco, E. Diseño In Silico de una Molécula con Propiedades Germicidas Inhibidora de la ADN Girasa de *Pseudomonas Aeruginosa*. Bachelor's Thesis, Universidad de San Carlos de Guatemala, Guatemala City, Guatemala, 2017.
32. Kampranis, S.C.; Maxwell, A. The DNA gyrase-quinolone complex. ATP hydrolysis and the mechanism of DNA cleavage. *J. Biol. Chem.* **1998**, *273*, 22615–22626. [CrossRef]
33. Susanta, S.; Surendra, P.; Ashish, P. In-silico identification and molecular docking studies of quinolone resistance determining region (QRDR) of *E. coli* DNA gyrase-a with ofloxacin schiff bases. *Int. J. PharmTech Res.* **2013**, *5*, 1794–1803.
34. Collin, F.; Karkare, S.; Maxwell, A. Exploiting bacterial DNA gyrase as a drug target: Current state and perspectives. *Appl. Microbiol. Biotechnol.* **2011**, *92*, 479–497. [CrossRef]
35. Vashist, J.; Vishvanath; Kapoor, R.; Kapil, A.; Yenamalli, R.; Subbarao, N.; Rajeswari, M.R. Interaction of nalidixic acid and ciprofloxacin with wild type and mutated quinolone-resistance-determining region of DNA gyrase A. *Indian J. Biochem. Biophys.* **2009**, *46*, 147–153.
36. Medapi, B.; Meda, N.; Kulkarni, P.; Yogeewari, P.; Sriram, D. Development of acridine derivatives as selective Mycobacterium tuberculosis DNA gyrase inhibitors. *Bioorg. Med. Chem.* **2016**, *24*, 877–885. [CrossRef]
37. Cramariuc, O.; Rog, T.; Javanainen, M.; Monticelli, L.; Polishchuk, A.V.; Vattulainen, I. Mechanism for translocation of fluoroquinolones across lipid membranes. *Biochim. Biophys. Acta Biomembr.* **2012**, *1818*, 2563–2571. [CrossRef] [PubMed]
38. Orero, A.; Cantón, E.; Pemán, J.; Gobernado, M. Penetración de los antibióticos de los polimorfos nucleares humanos, con especial referencia a las quinolonas. *Rev. Española Quim.* **2002**, *15*, 1–14.
39. Vaden, A.; Lotz, C.; Ortiz, J.; Lamour, V. Cryo-EM structure of the complete *E. coli* DNA gyrase nucleoprotein complex. *Nat. Commun.* **2019**, *10*, 4935–4947.
40. Brown, S. *Bioinformatics. A Biologist's Guide to Biocomputing and the Internet*; Eaton Publishing: New York, NY, USA, 2000.
41. Homologia. Available online: <http://webs.ucm.es/info/biomol2/bioquimicaI/WTA/Homologia.html> (accessed on 7 September 2021).
42. Ochman, H. Evolución y Enfermedad: ¿Qué convirtió la “salmonella” en maléfica? *Métode Sci. Stud. J.* **2014**, *4*, 178–180.
43. Contreras, B.; Yruea, I. Alineamiento de Secuencias, Estructura Secundaria, Desorden y Filogenias de Proteínas Didactic Material. Available online: <http://hdl.handle.net/10261/117608> (accessed on 7 September 2021).
44. Rodríguez, E. *Alineamiento de Pares de Secuencias*; Instituto Politécnico Nacional: Mexico City, Mexico, 2013.
45. Biopolimeros. Available online: http://facultatciencias.uib.cat/prof/josefa.donoso/campus/modulos/modulo4/modulo4_13.htm (accessed on 12 July 2021).
46. Aykul, S.; Martinez, E. Determination of half-maximal inhibitory concentration using biosensor-based protein interaction analysis. *Anal. Biochem.* **2017**, *508*, 97–103. [CrossRef]
47. Beltrán, Y.; Rojas, J.A.; Morales, I.; Morris, H. Acoplamiento molecular de compuestos fenólicos de *Pleurotus ostreatus* con proteínas del balance redox. *Rev. Cuba. Química* **2019**, *31*, 336–356.

48. Vallejo, D. Interacciones Eléctricas en Macromoléculas de Interés Biológico. Ph.D. Thesis, Universidad Nacional de La Plata, La Plata, Argentina, 2005.
49. Villacis, N. Estudios Bioinformáticos Sobre la Proteína Spike del SARS-CoV-2 para el Desarrollo de Posibles Inhibidores. Bachelor's Thesis, Universidad Técnica de Ambato, Ambato, Ecuador, 2021.
50. Spinosa, M.A. Caracterización Estructural y Docking Molecular en el Receptor Cannabinoide 2. Bachelor's Thesis, Universidad de Buenos Aires, Buenos Aires, Argentina, 2017.
51. Heinzlmann, G.; Gilson, M.K. Automation of absolute protein-ligand binding free energy calculations for docking refinement and compound evaluation. *Sci. Rep.* **2021**, *11*, 1–18. [[CrossRef](#)]
52. Baldiris, R.; Caicedo, D.; Velásquez, M.; Valdiris, V.; Vivas-Reyes, R. Docking molecular de inhibidores de actividad quinasa: Inhibición de la piridoxal quisana. *Cienc Salud Virtual* **2014**, *6*, 99–105. [[CrossRef](#)]
53. Sethi, A.; Joshi, K.; Sasikala, K.; Alvala, M. Molecular Docking in Modern Drug Discovery: In Principles and Recent Applications. In *Drug Discovery and Development—New Advances*; Gaitonde, V., Karmakar, P., Trivedi, A., Eds.; IntechOpen: London, UK, 2020; pp. 1–21.